

Semifluorinated Alkylphosphonic Acids Form High-Quality Self-Assembled Monolayers on Ag-Coated Yttrium Barium Copper Oxide Tapes and Enable Filamentization of the Tapes by Microcontact Printing

Chul Soon Park,^{†,‡} Han Ju Lee,^{†,‡} Dahye Lee,^{†,§} Andrew C. Jamison,^{†,‡} Eduard Galstyan,[†] Wanda Zagodzdzon-Wosik,^{||} Herbert C. Freyhardt,[†] Allan J. Jacobson,^{†,‡} and T. Randall Lee^{*,†,‡}

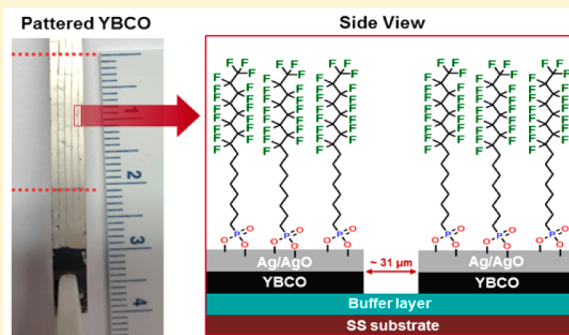
[†]Texas Center for Superconductivity and [‡]Department of Chemistry, University of Houston, 4800 Calhoun Road, Houston, Texas 77204, United States

[§]Materials Science and Engineering Program, University of Houston, Houston, Texas 77204, United States

^{||}Department of Electrical and Computer Engineering, University of Houston, Houston, Texas 77004-4005, United States

Supporting Information

ABSTRACT: A custom-designed semifluorinated phosphonic acid, (9,9,10,10,11,11,12,12,13,13,14,14,15,15,16,16-heptadecafluorohexadecyl)phosphonic acid (F8H8PA), and a normal hexadecylphosphonic acid (H16PA) were synthesized and used to generate self-assembled monolayers (SAMs) on commercially available yttrium barium copper oxide (YBCO) tapes. In this study, we wished to evaluate the effectiveness of these monolayer films as coatings for selectively etching YBCO. Initial films formed by solution deposition and manual stamping using a non-patterned polydimethylsiloxane stamp allowed for a comparison of the film-formation characteristics. The resulting monolayers were characterized by X-ray photoelectron spectroscopy (XPS), contact angle goniometry, and polarization modulation infrared reflection absorption spectroscopy (PM-IRRAS). To prepare line-patterned (filamentized) YBCO tapes, standard microcontact printing (μ -CP) procedures were used. The stamped patterns on the YBCO tapes were characterized by scanning electron microscopy (SEM) before and after etching to confirm the effectiveness of the patterning process on the YBCO surface and energy-dispersive X-ray spectroscopy (EDX) to obtain the atomic composition of the exposed interface.



INTRODUCTION

Self-assembled monolayers (SAMs) of organic amphiphilic adsorbates on metal and metal oxide substrates have been thoroughly studied and developed.^{1,2} This form of surface modification is used for corrosion protection, boundary lubrication, and anti-fouling applications.^{3–5} SAMs formed from thiol-based adsorbates on gold and alkylsilanes on silica are the best known and most widely studied SAMs.^{6–8} In contrast, monolayers formed from adsorbates with phosphorus headgroups are less well-known, but studies have shown that long-chain alkyl phosphonic acids or alkyl phosphoric acids form robust and well-anchored monolayers on a variety of metal oxide surfaces.^{9–13} These phosphorus-based acids form covalent bonds on the metal substrates via a condensation reaction between the hydroxyl moieties bound to phosphorus and the hydroxyl groups on the substrate.^{12,14} Notably, researchers have found that phosphonic acids form more thermally stable adsorbates than comparable phosphoric acids.¹⁰ Therefore, in this investigation, we have prepared SAMs from phosphonic acids in efforts to generate protective

coatings during the templated patterning of superconducting yttrium barium copper oxide (YBCO) tapes.

For coated conductors (CCs), high alternating current (ac) loss has remained a concern for applications in power- and electro-technologies involving rotating devices, cables and transformers.^{15,16} High ac losses for these components are related to their high aspect ratio, with hysteretic ac losses in perpendicular fields, which represent a significant portion of the total ac loss. However, the ac loss of a CC tape can be reduced by narrow filamentization.^{17–20} For filamentization of CCs, diverse techniques have been employed, such as laser scribing, photolithography, and ion-beam etching.^{21–23} However, conventional photolithography techniques are costly, even though the technique has been continuously improved to reach deep submicron or even nm resolution. While ion-beam lithography can be used to prepare sub-micrometer patterns on

Received: June 24, 2016

Revised: July 27, 2016

Published: August 2, 2016

solid substrates, it requires expensive systems to generate the patterns and is time-consuming. To overcome these drawbacks and limitations, Whitesides and co-workers devised an alternative technique known as microcontact printing (μ -CP), which is a “soft lithography” technique.²⁴ The technique of μ -CP printing has been used in a variety of micro-/nanofabrication and biotechnological applications.^{25–27} The method is fast and inexpensive, affording both flat and curved patterned surfaces over large areas in a single step, producing high-quality results that were not accessible using the aforementioned conventional methods.^{28,29}

In this report, we synthesized two adsorbate molecules and characterized their ability to form monolayers on silver-coated YBCO substrates; the molecules are hexadecylphosphonic acid (H16PA) and (9,9,10,10,11,11,12,12,13,13,14,14,15,15,16,16,16-heptafluorohexadecyl)phosphonic acid (F8H8PA). Figure 1 shows their structure. To determine the composition,

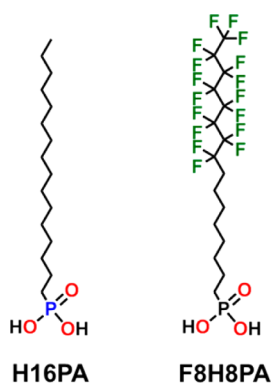


Figure 1. Structures of the adsorbates H16PA and F8H8PA used to form SAMs on silver-coated YBCO tapes.

structure, and quality of the films produced from these adsorbates, we prepared SAMs from each molecule on silver-coated YBCO surfaces using a non-patterned polydimethylsiloxane (PDMS) stamp via a manual stamping method and a solution deposition procedure (the “dipping method”). The resulting SAMs were examined using X-ray photoelectron spectroscopy (XPS), polarization modulation infrared reflection absorption spectroscopy (PM-IRRAS), and contact angle goniometry. The H16PA SAM was used in this study as reference system. For the filamentization of the YBCO superconducting tape, a line-patterned PDMS stamp was employed to form well-defined line patterns on the YBCO surfaces. The YBCO tape that was patterned with F8H8PA and subsequently etched (filamentized) was characterized using scanning electron microscopy (SEM) and energy-dispersive X-ray spectroscopy (EDX).

EXPERIMENTAL SECTION

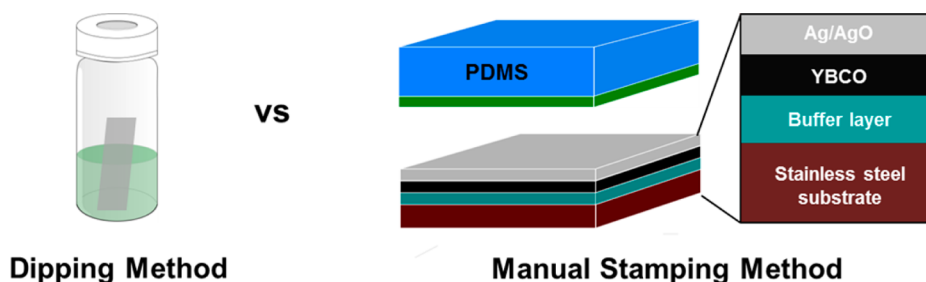
Materials. 1-Bromohexadecane, triethyl phosphite (98%), zinc (Zn), azobis(isobutyronitrile) (AIBN), methanesulfonyl chloride (MsCl), triethylamine (Et₃N), lithium bromide (LiBr), and bromotrimethylsilane (TMSBr) were purchased from Sigma-Aldrich. 7-Octen-1-ol was purchased from TCI. Perfluoro-1-iodooctane [CF₃(CF₂)₇I] was purchased Alfa Aesar. Most of the solvents and the reagent acetic acid (AcOH) were acquired from Sigma-Aldrich, while acetone was purchased from Mallinckrodt Chemicals. Hydrochloric acid (HCl), tetraammonium hydroxide (NH₄OH), and hydrogen peroxide (H₂O₂) were purchased from Macron Fine Chemicals, and phosphoric acid (H₃PO₄) was purchased from EM Science. Poly(dimethylsiloxane) (PDMS, Sylgard 184) was obtained from Dow Corning. The anhydrous ethanol (EtOH) used to develop the SAMs came from Decon Laboratories, Inc. Water was purified to a resistivity of 18 M Ω cm using an Academic Milli-Q water system (Millipore Corporation) and filtered through a 0.22 μ m membrane filter before use. The silver-coated YBCO tape was generously donated by Bruker Energy & Supercon Technologies. Adsorbates H16PA³⁰ and F8H8PA³¹ were prepared as described in the literature.

Deposition of SAMs Formed from H16PA and F8H8PA by the Dipping Method. We prepared monolayers with H16PA and F8H8PA to compare the quality of the monolayers produced via the dipping method versus the manual stamping method, as illustrated in Scheme 1. For the dipping method, the silver-coated YBCO surface was treated with oxygen plasma, followed by placing samples of the YBCO tape in 5 mM ethanolic solutions of each of the two adsorbates for an exposure time of at least 24 h. After 24 h, we removed the tapes from the vial with tweezers and then fixed them on a flat substrate. We then rinsed the tapes with ethanol, dried them with pure nitrogen gas, and transferred them to an oven at 80 °C for 20 min. After removal from the oven, we allowed the YBCO tapes to cool for 10 min and then washed them with ethanol before characterization.

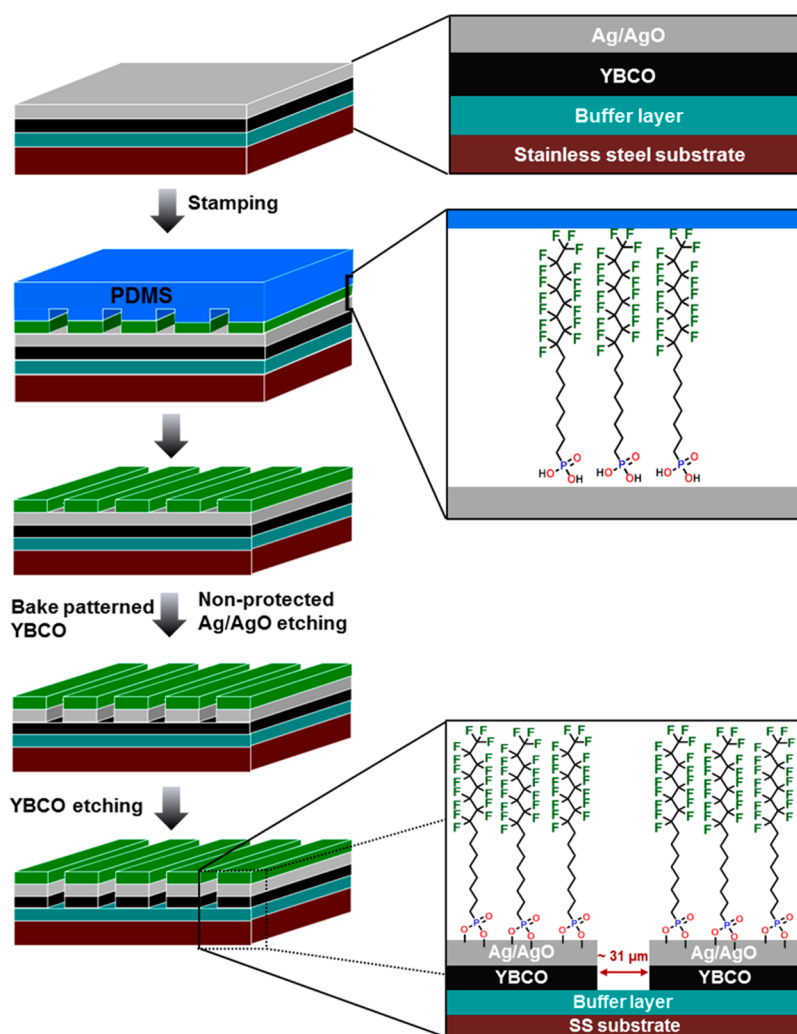
Deposition of SAMs Formed from H16PA and F8H8PA by Manual Stamping. In initial experiments, we performed μ -CP using a non-patterned PDMS stamp covered with 5 mM ethanolic F8H8PA solution with contact between the stamp and the tape maintained for 1 min. The freshly stamped YBCO tape was then transferred to an oven at 80 °C and heated for 20 min. Afterward, the YBCO tape was maintained at room temperature. The sample surface was washed with ethanol and dried with pure nitrogen gas before each characterization procedure.

Fabrication of PDMS Stamps. Sylgard 184 (30 g) was weighed in a plastic cup, and then 3 g of curing agent were added. The mixture was mixed vigorously for 10 min until the blended materials produced copious bubbles. The plastic cup was placed in a desiccator for 1 h under high vacuum to remove the bubbles from the mixture. After 1 h, we poured the freshly prepared PDMS slowly into a plastic Petri dish that contained either no mask or a pre-patterned mask on a silicon wafer, stopping when the PDMS layer was about 3 cm deep. The Petri dish was then placed in an oven and cured at 80 °C for 1 h. After cooling, we cut out the pattern with a sharp scalpel to isolate the patterned PDMS stamp, which was then stored in EtOH. The length of patterns of the PDMS stamp was 2.8 cm, and the patterned PDMS stamp contained four lines having a width of \sim 25 μ m each.

Scheme 1. Dipping and Manual Stamping Methods to Prepare Monolayers on YBCO Surfaces



Scheme 2. Preparation of Line-Patterned YBCO Tapes



Preparation of Patterned YBCO Tape Protected with a F8H8PA SAM. To produce the filamentized YBCO tapes, we created the patterns on the silver-coated YBCO tapes with F8H8PA using the procedure shown in Scheme 2. First, we covered the PDMS stamp with 5 mM F8H8PA in EtOH using a cotton swab, followed by drying with pure nitrogen gas. Next, we placed the F8H8PA-covered surface of PDMS in contact with the silver surface of YBCO for 1 min and then heated the tape in an oven at 80 °C for 40 min to generate covalent bonds between the phosphonate adsorbates and the silver oxide surface through condensation reactions. After 20 min, the surface-patterned YBCO tapes were washed with ethanol and placed in a silver etchant (30:1:1 H₂O/NH₄OH/H₂O₂) for 5 min to remove the non-protected silver. Afterward, the YBCO tapes were transferred to a more highly concentrated silver etchant (30:1.6:1.6 H₂O/NH₄OH/H₂O₂), at which point the black etched lines associated with exposed YBCO could be observed with the eye. The YBCO tapes were then dipped into the YBCO etchant (3% H₃PO₄ in H₂O) for 5 min. Finally, the line-patterned YBCO tapes were washed with ethanol, dried with nitrogen gas, and prepared for characterization. As shown in Scheme 2, the tapes are composed of the silver-coated YBCO, which were epitaxially grown on a buffer layer that contains CeO₂ and ZrO₂; these materials provide an insulating protective barrier between YBCO and the stainless-steel substrate.

RESULTS AND DISCUSSION

Analysis of the X-ray Photoelectron Spectra. The characteristic X-ray photoelectron spectra from the SAMs

derived from H16PA and F8H8PA are displayed in panels A and B of Figure 2, respectively. XPS data can be used to verify the presence of each of the key detectable elements present in the adsorbate structures. The SAMs derived with H16PA and F8H8PA possess hydrocarbons (C 1s), phosphate oxygens (O 1s), and phosphorus (P 2p) in common, as shown in the spectra in Figure 2. However, unlike the SAMs formed with H16PA, the F8H8PA SAMs also exhibit peaks associated with the CF₃ carbon (C 1s, ~293 eV), the CF₂ carbons (C 1s, ~290.9 eV), and the fluorine atoms (F 1s, ~688.4 eV).^{32,33} For all monolayers, the peak for the binding energy (BE) of Ag is used as a reference, as shown in panels A-1 and B-1 of Figure 2, consistent with prior work.³⁴ Importantly, we have compared the relative packing density of the SAMs based on the peak position of the C 1s BE; several previous studies have demonstrated the sensitivity of the C 1s BE peak position within the framework of the relative coverage of adsorbates on the surfaces.^{35,36} For the monolayers derived from H16PA, the peak for C 1s appears at ~284.6 eV for the monolayers formed from both dipping and manual stamping, as shown in Figure 2A-2. According to these results, the packing densities of the monolayers derived from H16PA using the two approaches are equivalent. Similarly, the C 1s (CH₂) peak for the SAMs formed from F8H8PA appear at ~284.3 eV, and the F 1s peaks appear at ~688.4 eV for both methods. These results suggest

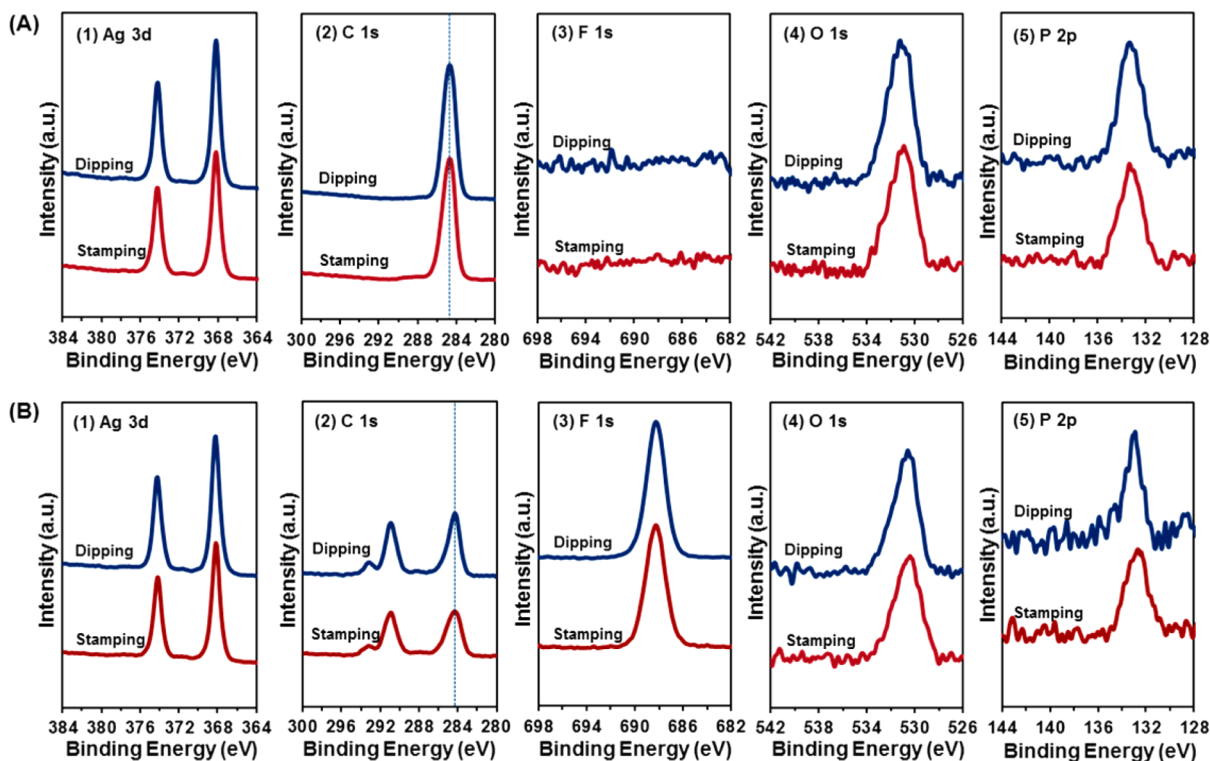


Figure 2. X-ray photoelectron spectra for the (1) Ag 3d, (2) C 1s, (3) F 1s, (4) O 1s, and (5) P 2p spectral regions of the films derived from (A) H16PA and (B) F8H8PA for films prepared by the dipping method (dark blue) or manual stamping (dark red).

that the packing and quality of the monolayers derived from dipping and manual stamping are probably comparable. We note also that the C 1s (CH_2) peaks in the SAMs derived from both H16PA and F8H8PA are sharp, which is consistent with monolayer formation for both adsorbates; more specifically, the C 1s peaks in multilayer films are broad due to differential surface charging within the multilayer.^{14,37}

Nevertheless, we were concerned that the C 1s (CH_2) peaks for the monolayers produced by manual stamping and the BE peak positions appear at ~ 284.6 and ~ 284.3 eV for H16PA and F8H8PA, respectively. Such a shift in BE likely correlates to a change in the packing density of the alkyl chains on the silver oxide surface, and it can be rationalized that the fluorinated chains having larger van der Waals diameters than the hydrocarbon chains would occupy a larger space on the surface.^{38–40} A lower C 1s BE has commonly been interpreted to indicate that a positive charge can be more easily discharged in a loosely packed SAM, owing to a reduction in its effectiveness as an insulator.^{41,42} According to the results obtained here, the monolayer derived from F8H8PA is plausibly less densely packed than that derived from H16PA. A comparison of panels A-3 and B-3 of Figure 2 illustrates the fluorine content in only the F8H8PA SAM as expected. The X-ray photoelectron spectra in panels A-4 and A-5 and B-4 and B-5 of Figure 2 are consistent with a model in which the dipping and stamping methods afford films of comparable chemical constitution and character.

Notably, the O 1s region can be used to verify the covalent bonding between the phosphonic acids and the silver coating of YBCO for the manual stamping procedure used to form patterns. Panels A and B of Figure 3 show the deconvolution of the peaks in the O 1s region for the bulk adsorbates and SAMs derived from each adsorbate: (A) H16PA and (B) F8H8PA. As

shown in Figure 3A-2 for the monolayer derived from H16PA, the O 1s peak contains two major components: a peak at ~ 532.2 eV and a peak at ~ 530.8 eV. These peaks are assigned to P–OH and P=O of the phosphonate group, respectively. For the F8H8PA SAMs, the O 1s deconvolution reveals peaks at ~ 531.9 and ~ 530.5 eV for P–OH and P=O, respectively (see Figure 3B-2). These values seem reasonable when compared to values found in the literature, although the peak positions shift somewhat as a function of the substrate.^{11,33–35,39} Panels A-1 and B-1 of Figure 3 show that the P–OH species dominate the composition of the O 1s peaks for bulk H16PA and F8H8PA; however, the P=O species dominate the O 1s region for SAMs derived from H16PA and F8H8PA by the manual stamping method (see panels A-2 and B-2 of Figure 3). These results are consistent with SAMs derived from similar adsorbate/substrate combinations.³⁹ When taken as a whole, these results can be interpreted to indicate that the manual stamping method generates good quality monolayer films from phosphonate adsorbates that are comparable to those obtained by the dipping method.

To compare further the quality of the monolayers, we evaluated the ratio of the integrated areas under the binding energy peaks for C/Ag, P/Ag, and F/Ag between the two deposition methods, obtaining the results shown in Figure S2 of the Supporting Information. For monolayers derived from H16PA using dipping and stamping, the ratios for C/Ag are 0.300 and 0.310, respectively; the ratios for P/Ag are 0.018 for both monolayers (see Figure S2A of the Supporting Information). According to these results, the packing densities of the H16PA monolayers derived from two approaches are similar. For the monolayers formed from F8H8PA, the ratios (C/Ag, P/Ag, and F/Ag) are roughly the same between dipping and manual stamping (see Figure S2B and Table S1 of

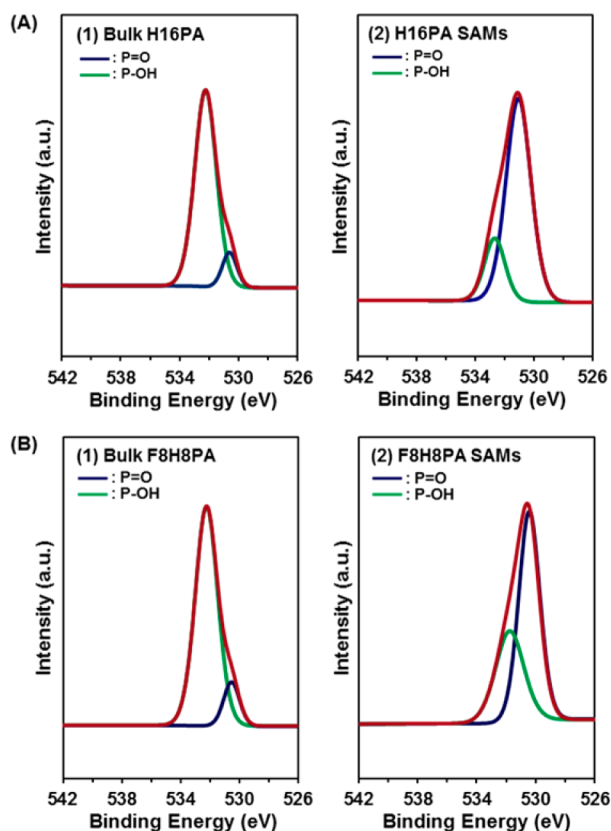


Figure 3. Deconvolution of the peaks in the O 1s region of the XPS spectra for (A) (1) bulk H16PA and (2) SAMs formed from H16PA and (B) (1) bulk F8H8PA and (2) SAMs formed from F8H8PA. The displayed data are from SAMs formed using the manual stamping method.

the Supporting Information). Importantly, the values for C/Ag and P/Ag for the monolayers derived from F8H8PA are approximately half that of the H16PA monolayers, which can be rationalized on the basis that the molecular packing densities of the monolayers derived from F8H8PA are less than those of the monolayers derived from H16PA, a result that is consistent with the XPS data and analysis described in the preceding section.

Contact Angle Measurements. Panels A and B of Figure 4 show the advancing contact angles (θ_a) and receding contact angles (θ_r) of water on monolayers derived from H16PA and

F8H8PA using the dipping and manual stamping methods. Contact angle hysteresis ($\Delta\theta = \theta_a - \theta_r$) also provides insight into the interfacial properties of the films.⁴³ Figure 4A shows the advancing and receding contact angles of water on the monolayers derived from H16PA using the dipping and manual stamping methods ($\theta_a = 116^\circ$ and 115° , respectively, while θ_r is 100° for both surfaces).^{11,30} For these SAMs, the contact angle values and the hysteresis values ($\Delta\theta = 16^\circ$ and 15° , respectively) are consistent with comparably smooth, homogeneous surfaces and literature values for SAMs derived from phosphonic acids on aluminum.³⁰ For monolayers derived from F8H8PA (Figure 4B), the θ_a values for water were 127° and 125° for the dipping and stamping methods, respectively. These values are much higher than for the monolayers formed with H16PA, and the advancing contact angles are similar to SAMs derived from thiol-based adsorbates.⁴⁴ On the basis of these contact angle data, the F8H8PA SAMs are much less wettable than the H16PA SAMs, which suggests enhanced resistance of the F8H8PA SAMs toward water-based etchants in the fabrication of patterned YBCO tapes (*vide infra*). The receding contact angles, θ_r , for these surfaces for water were 112° and 109° , respectively, and the corresponding contact angle hystereses were 15° and 16° . These results collectively indicate that there is little or no difference in the quality of the films generated by the dipping versus manual stamping methods.

Analysis of the PM-IRRAS Spectra. Surface infrared spectroscopy can be useful to characterize the general alkyl chain conformational order of SAMs derived from adsorbates with extended alkyl chains.⁴⁵ Because well-packed and ordered alkyl chain assemblies are organized in their lowest energy conformations, the degree of order for organic monolayers and any similarly structured films that rely on van der Waals attractions between long alkyl chains to stabilize the assembly can be evaluated by the band position of the antisymmetric methylene C–H stretching vibration ($\nu_a^{\text{CH}_2}$) obtained using PM-IRRAS.⁴⁶ The band positions of $\nu_a^{\text{CH}_2}$ for the SAMs derived from H16PA and F8H8PA using the dipping and manual stamping methods are shown in panels A and B of Figure 5, respectively. In Figure 5A, the band positions of $\nu_a^{\text{CH}_2}$ for the SAMs derived from H16PA are both at 2916 cm^{-1} , which is consistent with the value found for this adsorbate on aluminum.³⁰ According to these results, the conformational order of the monolayers formed using these two methods are the same. Figure 5B shows that the SAMs formed from F8H8PA either by dipping or stamping also have $\nu_a^{\text{CH}_2}$ bands

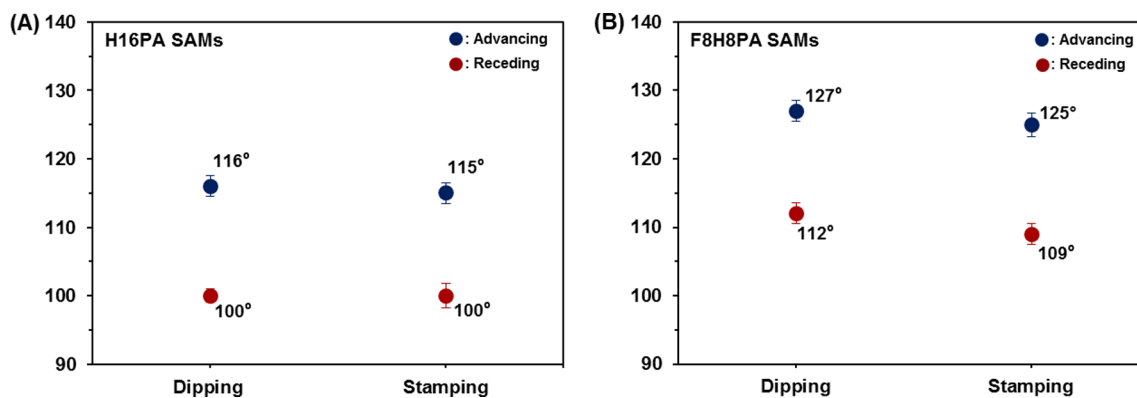


Figure 4. Advancing (blue circles) and receding (red circles) contact angles for water on monolayers derived from (A) H16PA and (B) F8H8PA for the dipping and manual stamping methods.

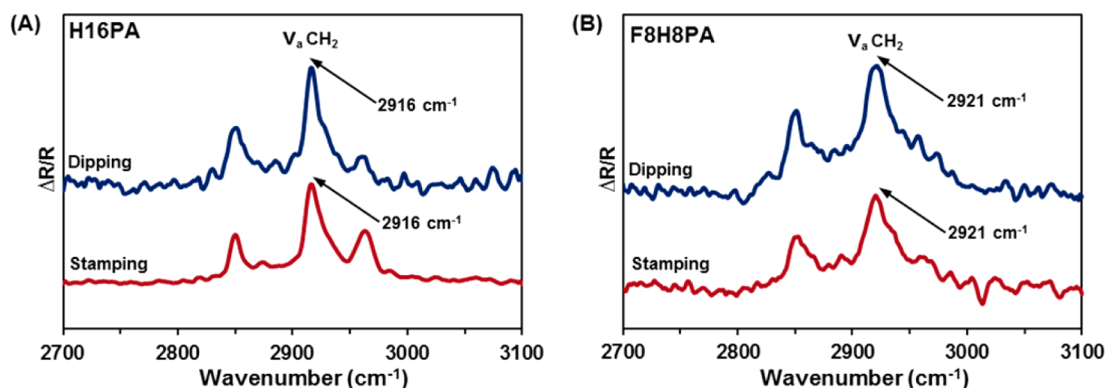


Figure 5. PM-IRRAS spectra of the C–H stretching region for the SAMs derived from (A) H16PA and (B) F8H8PA prepared by the dipping method (dark blue) or manual stamping (dark red).

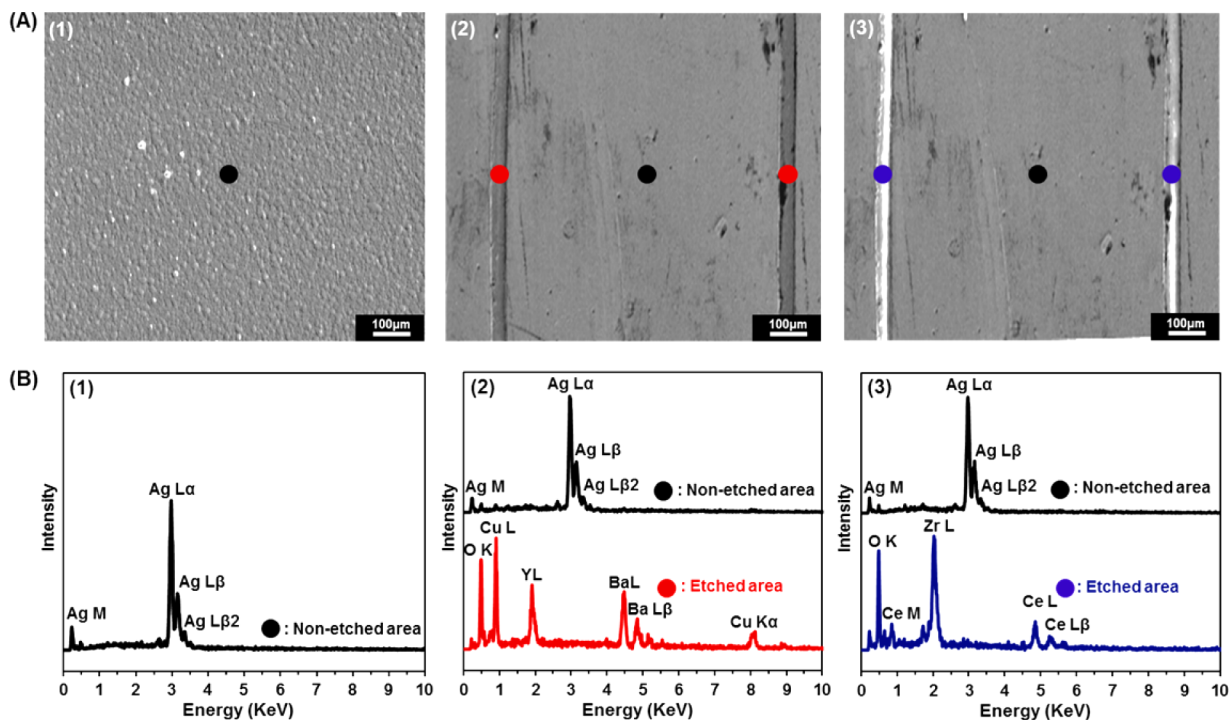


Figure 6. (A) SEM images and (B) EDX spectra of the YBCO tape (1) before etching, (2) after patterning and etching non-protected Ag, and (3) after etching uncoated YBCO. Dots on the SEM images are color-coded to indicate the data collection points for the EDX spectra as described in the text.

the same as each other, 2921 cm^{-1} . According to these results, the two deposition methods examined (dipping and manual stamping) generate monolayers of equivalent quality for both adsorbates examined in this study. Therefore, the results obtained using PM-IRRAS are consistent with those obtained by XPS and contact angle goniometry (*vide supra*).

Examination of the Etching Process. Figure 6 shows SEM images and EDX spectra for each step of the etching process. In Figure 6A-1, the SEM image shows the pristine silver-coated YBCO surface, and analysis by EDX (Figure 6B-1) shows only Ag on the area marked with a black dot. However, after patterning with F8H8PA and etching the unprotected area, we observed $\sim 31\text{ }\mu\text{m}$ line patterns that were etched (see the red dots in Figure 6A-2). For the silver-etched area, yttrium, barium, and copper (components of YBCO) were observed (see the red spectrum in Figure 6B-2). In contrast, the components of YBCO were not observed in the F8H8PA-

protected area (black spectrum in Figure 6B-2). We then etched YBCO with 3 wt % phosphoric acid solution. After etching the tape, there were no YBCO components observed by EDX, but Zr and Ce (elements in the underlying buffer surface) were observed (blue spectrum in Figure 6B-3). Furthermore, the non-etched, F8H8PA-protected area showed only Ag species (black spectrum in Figure 6B-3). From these results, we can conclude that the F8H8PA SAM efficiently protects the Ag surface and underlying YBCO from the etching process. Notably, initial attempts to generate similar patterns using H16PA were unsuccessful, as shown in Figure S1 of the Supporting Information, presumably due to the greater wettability (and thus greater permeability) of this SAM. Generally, SAMs generated from fluorocarbon adsorbates exhibit lower wettability and permeability toward water than hydrocarbon adsorbates;^{47,48} consequently, it follows that the

F8H8PA-protected areas are more resistant to water-based etchants.

CONCLUSION

The adsorbates, H16PA and F8H8PA, were successfully synthesized and used to form self-assembled monolayers on commercial silver-coated YBCO tapes using two deposition strategies: dipping and manual stamping. The monolayer films derived from H16PA and F8H8PA were characterized with XPS, contact angle goniometry, and PM-IRRAS to determine the quality of the monolayer films formed from these two methods. The collected data indicated that these methods produced films of equivalent quality. Analysis by XPS also demonstrated that the elemental composition of the films was consistent with that of the adsorbates. Accordingly, the packing density of the SAMs derived from F8H8PA were less than those of the H16PA SAMs, which could be attributed to the larger fluorinated chains occupying more space on the surface than the *n*-alkyl chains. Finally, SEM images and EDX data were used to verify that the silver-coated YBCO tapes were successfully patterned by microcontact printing using a patterned PDMS stamp and F8H8PA as the protective ink; in contrast, H16PA was ineffective for this purpose. These results set the stage for future studies of potential reduced ac loss afforded by filamentizing the YBCO tapes with subsequent annealing under oxygen as needed.⁴⁹

ASSOCIATED CONTENT

Supporting Information

The Supporting Information is available free of charge on the ACS Publications website at DOI: 10.1021/acs.langmuir.6b02368.

Additional XPS data for the SAMs formed from H16PA and F8H8PA, along with the instrumental procedures used to conduct the research in this report (PDF)

AUTHOR INFORMATION

Corresponding Author

*E-mail: trlee@uh.edu.

Notes

The authors declare no competing financial interest.

ACKNOWLEDGMENTS

The authors thank the National Science Foundation (CHE-1411265), the Robert A. Welch Foundation (Grants E-1320 and E-0024), and the Texas Center for Superconductivity at the University of Houston for generous support.

REFERENCES

- (1) Schreiber, F. Structure and Growth of Self-Assembling Monolayer. *Prog. Surf. Sci.* **2000**, *65*, 151–256.
- (2) Dubois, L. H.; Nuzzo, R. G. Synthesis, Structure, and Properties of Model Organic Surfaces. *Annu. Rev. Phys. Chem.* **1992**, *43*, 437–463.
- (3) Scherer, J.; Vogt, M. R.; Magnussen, O. M.; Behm, R. J. Corrosion of Alkanethiol-Covered Cu(100) Surfaces in Hydrochloric Acid Solution Studied by in-Situ Scanning Tunneling Microscopy. *Langmuir* **1997**, *13*, 7045–7051.
- (4) Houston, J. E.; Doelling, C. M.; Vanderlick, T. K.; Hu, Y.; Scoles, G.; Wenzl, I.; Lee, T. R. Comparative Study of the Adhesion, Friction, and Mechanical Properties of CF₃- and CH₃-Terminated Alkanethiol Monolayers. *Langmuir* **2005**, *21*, 3926–3932.

(5) Huang, C. J.; Wang, L. C.; Shyue, J. J.; Chang, Y. C. Developing Antifouling Biointerfaces Based on Bioinspired Zwitterionic Dopamine through pH-Modulated Assembly. *Langmuir* **2014**, *30*, 12638–12646.

(6) Nuzzo, R. G.; Allara, D. L. Adsorption of Bifunctional Organic Disulfides on Gold Surfaces. *J. Am. Chem. Soc.* **1983**, *105*, 4481–4483.

(7) Bain, C. D.; Troughton, E. B.; Tao, Y. T.; Evall, J.; Whitesides, G. M.; Nuzzo, R. G. Formation of Monolayer Films by the Spontaneous Assembly of Organic Thiols from Solution onto Gold. *J. Am. Chem. Soc.* **1989**, *111*, 321–335.

(8) Onclin, S.; Ravoo, B. J.; Reinhoudt, D. N. Engineering Silicon Oxide Surfaces Using Self-Assembled Monolayers. *Angew. Chem., Int. Ed.* **2005**, *44*, 6282–6304.

(9) Sinapi, F.; Forget, L.; Delhalle, J.; Mekhalif, Z. Formation and Characterization of Thin Films of H(CH₂)_x PO(OH)₂ on Polycrystalline Zinc Substrates. *Surf. Interface Anal.* **2002**, *34*, 148–154.

(10) Davies, P. R.; Newton, N. G. The Chemisorption of Organophosphorus Compounds at an Al(111) Surface. *Appl. Surf. Sci.* **2001**, *181*, 296–306.

(11) Spori, D. M.; Venkataraman, N. V.; Tosatti, S. G. P.; Durmaz, F.; Spencer, N. D.; Zurcher, S. Influence of Alkyl Chain Length on Phosphate Self-Assembled Monolayers. *Langmuir* **2007**, *23*, 8053–8060.

(12) Gnauck, M.; Jaehne, E.; Blaettler, T.; Tosatti, S.; Textor, M.; Adler, H. P. Carboxy-Terminated Oligo(ethylene glycol)-Alkane Phosphate: Synthesis and Self-Assembly on Titanium Oxide Surfaces. *Langmuir* **2007**, *23*, 377–381.

(13) Marcinko, S.; Fadeev, A. Y. Hydrolytic Stability of Organic Monolayers Supported on TiO₂ and ZrO₂. *Langmuir* **2004**, *20*, 2270–2273.

(14) Zhang, B.; Kong, T.; Xu, W.; Su, R.; Gao, Y.; Cheng, G. Surface Functionalization of Zinc Oxide by Carboxyalkylphosphonic Acid Self-Assembled Monolayers. *Langmuir* **2010**, *26*, 4514–4522.

(15) Chevtchenko, O.; Zuijderduin, R.; Smit, J.; Willén, D.; Lentge, H.; Thidemann, C.; Traeholt, C.; Melnik, I.; Geschiere, A. Low AC Loss in a 3 kA HTS Cable of the Dutch Project. *Phys. Procedia* **2012**, *36*, 1285–1289.

(16) Heydari, H.; Faghihi, F.; Aligholizadeh, R. A New Approach for AC Loss Reduction in HTS Transformer using Auxiliary Windings, Case Study: 25 kA HTS Current Injection Transformer. *Supercond. Sci. Technol.* **2008**, *21*, 015009.

(17) Amemiya, N.; Kasai, S.; Yoda, K.; Jiang, Z.; Levin, G. A.; Barnes, P. N.; Oberly, C. E. AC Loss Reduction of YBCO Coated Conductors by Multifilamentary Structure. *Supercond. Sci. Technol.* **2004**, *17*, 1464–1471.

(18) Carr, W. J., Jr.; Oberly, C. E. Filamentary YBCO Conductors for AC Applications. *IEEE Trans. Appl. Supercond.* **1999**, *9*, 1475–1478.

(19) Levin, G. A.; Barnes, P. N.; Kell, J. W.; Amemiya, N.; Jiang, Z.; Yoda, K.; Kimura, F. Multifilament YBa₂Cu₃O_{6+x}-Coated Conductors with Minimized Coupling Losses. *Appl. Phys. Lett.* **2006**, *89*, 012506.

(20) Zhang, Y.; Duckworth, R. C.; Ha, T. T.; List, F. A., III; Gouge, M. J.; Chen, Y.; Xiong, X.; Selvamaniack, V.; Polyanski, A. AC Loss Reduction in Filamentized YBCO Coated Conductors with Virtual Transverse Cross-Cuts. *IEEE Trans. Appl. Supercond.* **2011**, *21*, 3301–3306.

(21) Suzuki, K.; Matsuda, J.; Yoshizumi, M.; Izumi, T.; Shiohara, Y.; Iwakuma, M.; Ibi, A.; Miyata, S.; Yamada, Y. Development of a Laser Scribing Process of Coated Conductors for the Reduction of AC Losses. *Supercond. Sci. Technol.* **2007**, *20*, 822–826.

(22) Mishra, S. K.; Pathak, L. C.; Ray, S. K.; Kal, S.; Bhattacharya, D.; Lahiri, S. K.; Chopra, K. L. Lithographic Patterning of Superconducting YBCO Films. *J. Supercond.* **1992**, *5*, 445–449.

(23) Curtz, N.; Koller, E.; Zbinden, H.; Decroux, M.; Antognazza, L.; Fischer, Ø.; Gisin, N. Patterning of Ultrathin YBCO Nanowires Using a New Focused-Ion-Beam Process. *Supercond. Sci. Technol.* **2010**, *23*, 045015.

(24) Jackman, R. J.; Brittain, S. T.; Adams, A.; Wu, H.; Prentiss, M. G.; Whitesides, S.; Whitesides, G. M. Three-Dimensional Metallic Microstructures Fabricated by Soft Lithography and Microelectrodeposition. *Langmuir* **1999**, *15*, 826–836.

- (25) Buhl, M.; Vonhören, B.; Ravoo, B. J. Immobilization of Enzymes via Microcontact Printing and Thiol–Ene Click Chemistry. *Bioconjugate Chem.* **2015**, *26*, 1017–1020.
- (26) Graber, D. J.; Zieziulewicz, T. J.; Lawrence, D. A.; Shain, W.; Turner, J. N. Antigen Binding Specificity of Antibodies Patterned by Microcontact Printing. *Langmuir* **2003**, *19*, 5431–5434.
- (27) Ogihara, H.; Kibayashi, H.; Saji, T. Microcontact Printing for Patterning Carbon Nanotube/Polymer Composite Films with Electrical Conductivity. *ACS Appl. Mater. Interfaces* **2012**, *4*, 4891–4897.
- (28) Xue, C. Y.; Chin, S. Y.; Khan, S. A.; Yang, K. L. UV-Defined Flat PDMS Stamps Suitable for Microcontact Printing. *Langmuir* **2010**, *26*, 3739–3743.
- (29) Jackman, R. J.; Wilbur, J. L.; Whitesides, G. M. Fabrication of Submicrometer Features on Curved Substrates by Microcontact Printing. *Science* **1995**, *269*, 664–666.
- (30) Pellerite, M. J.; Dunbar, T. D.; Boardman, L. D.; Wood, E. J. Effects of Fluorination on Self-Assembled Monolayer Formation from Alkanephosphonic Acids on Aluminum: Kinetics and Structure. *J. Phys. Chem. B* **2003**, *107*, 11726–11736.
- (31) Trabelsi, S.; Zhang, S.; Zhang, Z.; Lee, T. R.; Schwartz, D. K. Semi-fluorinated Phosphonic Acids Form Stable Nanoscale Clusters in Langmuir-Blodgett and Self-Assembled Monolayers. *Soft Matter* **2009**, *5*, 750–758.
- (32) Paniagua, S. A.; Hotchkiss, P. J.; Jones, S. C.; Marder, S. R.; Mudalige, A.; Marrikar, F. S.; Pemberton, J. E.; Armstrong, N. R. Phosphonic Acid Modification of Indium-Tin Oxide Electrodes: Combined XPS/UPS/Contact Angle Studies. *J. Phys. Chem. C* **2008**, *112*, 7809–7817.
- (33) Wang, M.; Hill, I. G. Fluorinated Alkyl Phosphonic Acid SAMs Replace PEDOT:PSS in Polymer Semiconductor Devices. *Org. Electron.* **2012**, *13*, 498–505.
- (34) Xiao, F.; Liu, H.-G.; Lee, Y.-I. Formation and Characterization of Two-Dimensional Arrays of Silver Oxide Nanoparticles under Langmuir Monolayers of *n*-Hexadecyl Dihydrogen Phosphate. *Bull. Korean Chem. Soc.* **2008**, *29*, 2368–2372.
- (35) Biebuyck, H. A.; Bain, C. D.; Whitesides, G. M. Comparison of Organic Monolayers on Polycrystalline Gold Spontaneously Assembled from Solutions Containing Dialkyl Disulfides or Alkanethiols. *Langmuir* **1994**, *10*, 1825–1831.
- (36) Park, J. S.; Vo, A. N.; Barriet, D.; Shon, Y. S.; Lee, T. R. Systematic Control of the Packing Density of Self-Assembled Monolayers Using Bidentate and Tridentate Chelating Alkanethiols. *Langmuir* **2005**, *21*, 2902–2911.
- (37) Gouzman, I.; Dubey, M.; Carolus, M. D.; Schwartz, J.; Bernasek, S. L. Monolayer vs. Multilayer Self-Assembled Alkylphosphonate Films: X-ray Photoelectron Spectroscopy Studies. *Surf. Sci.* **2006**, *600*, 773–781.
- (38) Zorn, G.; Gotman, I.; Gutmanas, E. Y.; Adadi, R.; Salitra, G.; Sukenik, C. N. Surface Modification of Ti₄₅Nb Alloy with an Alkylphosphonic Acid Self-Assembled Monolayer. *Chem. Mater.* **2005**, *17*, 4218–4226.
- (39) Hoque, E.; DeRose, J. A.; Hoffmann, P.; Bhushan, B.; Mathieu, H. J. Alkylperfluorosilane Self-Assembled Monolayers on Aluminum: A Comparison with Alkylphosphonate Self-Assembled Monolayers. *J. Phys. Chem. C* **2007**, *111*, 3956–3962.
- (40) Bain, C. D.; Whitesides, G. M. Formation of Monolayers by the Coadsorption of Thiols on Gold: Variation in The Length of the Alkyl Chain. *J. Am. Chem. Soc.* **1989**, *111*, 7164–7175.
- (41) Ishida, T.; Nishida, N.; Tsuneda, S.; Hara, M.; Sasabe, H.; Knoll, W. Alkyl Chain Length Effect on Growth Kinetics of *n*-Alkanethiol Self-Assembled Monolayers on Gold Studied by X-Ray Photoelectron Spectroscopy. *Jpn. J. Appl. Phys.* **1996**, *35*, L1710–L1713.
- (42) Ishida, T.; Hara, M.; Kojima, I.; Tsuneda, S.; Nishida, N.; Sasabe, H.; Knoll, W. High Resolution X-ray Photoelectron Spectroscopy Measurements of Octadecanethiol Self-Assembled Monolayers on Au(111). *Langmuir* **1998**, *14*, 2092–2096.
- (43) Folkers, J. P.; Laibinis, P. E.; Whitesides, G. M. Self-Assembled Monolayers of Alkanethiols on Gold: Comparisons of Monolayers Containing Mixtures of Short and Long-chain Constituents with CH₃ and CH₂OH Terminal Groups. *Langmuir* **1992**, *8*, 1330–1341.
- (44) Yuan, Y.; Yam, C. M.; Shmakova, O. E.; Colorado, R., Jr.; Graupe, M.; Fukushima, H. H.; Moore, H. J.; Lee, T. R. Solution-Phase Desorption of Self-Assembled Monolayers on Gold Derived From Terminally Perfluorinated Alkanethiols. *J. Phys. Chem. C* **2011**, *115*, 19749–19760.
- (45) Perry, S. S.; Somorjai, G. A. Characterization of Organic Surfaces. *Anal. Chem.* **1994**, *66*, 403A–415A.
- (46) Snyder, R. G.; Hsu, S. L.; Krimm, S. Vibrational Spectra in the C–H Stretching Region and the Structure of the Polymethylene Chain. *Spectrochim. Acta, Part A* **1978**, *34*, 395–406.
- (47) Genzer, J.; Efimenko, K. Creating Long-Lived Superhydrophobic Polymer Surfaces Through Mechanically Assembled Monolayers. *Science* **2000**, *290*, 2130–2133.
- (48) Li, X.; Li, J.; Eleftheriou, M.; Zhou, R. Hydration and Dewetting near Fluorinated Superhydrophobic Plates. *J. Am. Chem. Soc.* **2006**, *128*, 12439–12447.
- (49) Kim, M.; Freyhardt, H. C.; Lee, T. R.; Jacobson, A. J.; Galstyan, E.; Usoskin, A.; Rutt, A. Filamentization of YBCO Coated Conductors by Microcontact Printing. *IEEE Trans. Appl. Supercond.* **2013**, *23*, 6601304.